TCM - RUST WURZBURG 1992

Correlation and dimensional analysis of density fluctuations on CASTOR Tokamak

J. Stöckel, L. Kryška, J. Holakovský, J. Petržílka, V. Svoboda, F. Žáček
Institute of Plasma Physics, P.O.B. 17, 182 11 Prague, Czechoslovakia

Abstract

Regimes with reduced level of edge fluctuations are investigated on the CASTOR tokamak:

- Lower Hybrid Current Drive (LHCD) regime.
- Edge Plasma Polarization (EP) regime. The radial electric field is produced by means of a biased electrode immersed into the edge plasma.

The particle confinement improves only for LHCD, in spite of the fact that the density fluctuations are reduced in both cases. This suggests that the role of edge fluctuations in the global confinement is more complex then it is generally assumed.

At the same time, the correlation and dimensional analysis of fluctuation data indicates significant changes in character of the density fluctuations. Namely:
1) The autocorrelation time in the rest (convected) frame increases and
2) the fluctuations are more stochastic (closer to the white noise) when the particle confinement improves.

Key words: tokamak, confinement, fluctuations, dimensionality

1 Introduction

The electrostatic fluctuations are generally assumed to be important for explanation of the anomalous particle and energy losses in tokamaks [1], as shown schematically in the following diagram:

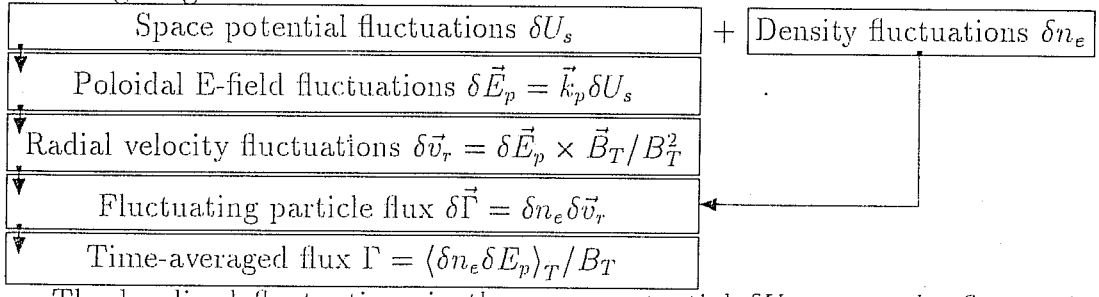

The localized fluctuations in the space potential δU_s create the fluctuations of the poloidal electric field $\delta \vec{E}_p = \vec{k}_p \delta U_s$ ($\vec{k}_p$ - is the poloidal wavenumber of U_s-fluctuations). Due to the cross-field drift $\vec{E}_p \times \vec{B}_T$, this leads to fluctuations in the radial velocity of the plasma particles δv_r and consequently to the fluctuations in the radial particle flux $\delta\Gamma$. It has been shown experimentally that the time averaged flux Γ has outwards direction at the plasma edge. Moreover, at the last closed flux surface (LCFS), the fluctuation-induced flux $\Gamma(a)$ is comparable with the particle outflux·determined from the global particle balance.

[1] P.C. Liewer: Nucl. Fusion, 25, 1985,543

The link between the edge electrostatic fluctuations and the global confinement was demonstrated in several experiments.

An increase of the global particle confinement time τ_p at lower hybrid current drive (LHCD) has been observed on VERSATOR [2] (by a factor of 2) and WT-3 [3] (by a factor of about 1.5) tokamaks at $P_{LH} \leq P^o_{OH}$ and low densities, but no reasonable explanation has been proposed. An attempt to explain this phenomenon in terms of reduction of the edge electrostatic fluctuations was recently supported by LHCD experiments on the CASTOR [4] and ASDEX [5] tokamaks. However, the mechanismus behind the reduction of the fluctuations in LHCD remains quite unclear.

Experiments with a strong NBI heating and with the edge plasma polarization (e.g. CCT [6], HYBTOK-II [7]) have demonstrated that non-ambipolar fluxes accros the plasma edge may induce a transition to regimes with the improved confinement (H-mode). Damping of the edge fluctuations, observed in these experiments, is explained by an enhanced shear of the poloidal rotation due to a modification of the radial electric field.

In addition, the simultaneous improvement of particle confinement and the reduction of fluctuations was recently reported from STOR-M [8] tokamak in regimes with a fast modification of the current density profile.

Aim of this contribution is to contribute to these investigations. Two regimes with a reduced fluctuations are arranged on CASTOR tokamak and compared in terms of particle confinement. The correlation and dimensional analysis of fluctuation data are performed under the same discharge conditions.

2 Experimental arrangement

Schematic arrangement of experiments with reduced density fluctuations, performed on the CASTOR tokamak ($R = 40\ cm, a = 8.5\ cm, I_p = 12\ kA, B_t = 1\ T, \bar{n}_e \leq 1 \cdot 10^{19} m^{-3}$), is shown in Fig. 1:

1. The regime with the lower hybrid current drive (LHCD). In this case, the lower hybrid wave ($f = 1.25\ GHz, P_{LH} < 40\ kW$) is launched into the plasma during the quasistationary phase of the discharge by means of a multijunction waveguide grill.

2. The regime with the edge plasma polarization (EP). In this case, a radial electric field is created at the plasma edge by biasing of an auxiliary electrode immersed into the edge plasma. We use a graphite electrode (1cm in length, 1cm in diameter) located at the top of the torus at $r/a = 0.8$ and biased by a modulator ($U < 300V, I < 100A, \tau < 40ms$).

The experiment is equipped by a set of diagnostics for the determination of the global particle confinement time and characterization of edge fluctuation.

[2] S.C. Luckhardt et al: Phys. Fluids, 29(6), 1986, 1985
[3] M. Nakamura et al: Nucl. Fusion, 31, 1991, 1485
[4] J. Stöckel et al:Plasma Phys. and Contr. Nucl. Fus. Research, 1988, Vol.1, p.359
[5] J. Stöckel, F.X. Söldner et al: Report IPP 1/268, Garching, March 1992
[6] R.J. Taylor et al: Phys. Rew. Letters, 63,1989,No.21, p.2365
[7] S. Takamura et al: IEEE Trans. on Plasma Sci. 19,1991,No.5
[8] A. Hirose: IAEA TCM on Research Using Small Tokamaks, Hefei, October 1991

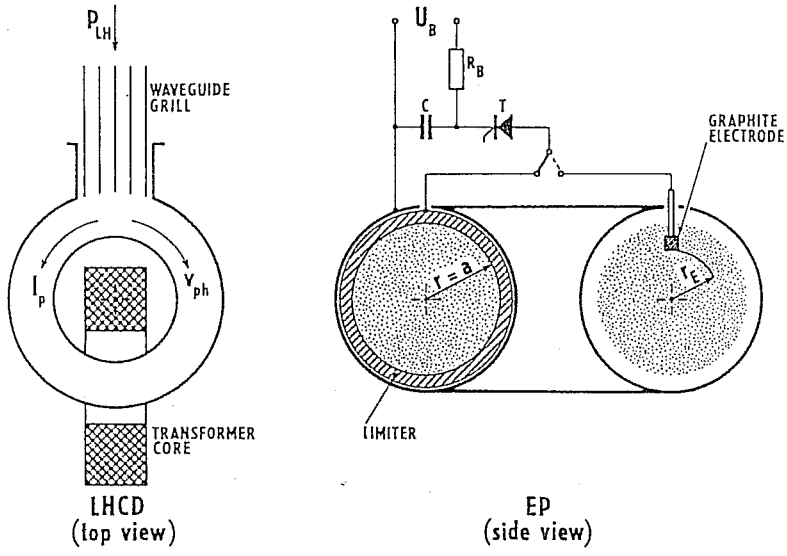

Figure 1: Schematic arrangement of the LHCD and EP experiments.

Global particle confinement:
The evolution of the global particle confinement time τ_p can be evalulated from the radial density profile (estimated by means of the two-channel microwave interferometer) and H_α - intensities (monitored at different toroidal locations).

Edge density fluctuations: The character of the density fluctuations at the plasma edge was deduced from fluctuating signals from a double Langmuir probe located at the equatorial plane of the torus opposit to the waveguide grill and in the same diagnostic section as the graphite electrode. The tips of the probe, denoted as A and B, were oriented in the poloidal direction, the distance between them being $\Delta = 4.5mm$. The temporal evolution of the square root value of the density fluctuations during a shot was monitored by the analog correlator.

Furthermore, the fluctuating part of the ion saturation current was digitized by the 10 bit A/D converter (with the sampling rate 0.2 $\mu s/sample$) in two blocks à 4 kByte. The first block was stored during the ohmic phase, while the second block contains data in the LHCD or EP phases.

Correlation functions:
To compare the fluctuations quantitatively in different regimes, we evaluate the correlation functions:

$$C_{AB}(t_d) = \lim_{T\to\infty} \frac{1}{T} \int_0^T f_A(t) f_B(t - t_d) dt \quad ,$$

where f_A, f_B are the fluctuating signals from the tips A and B, t_d is a time delay.

An example of the autocorrelation function ($A \equiv B$), shown in Fig. 2a, demonstrates our choise of the autocorrelation time τ_c^{lab} and the range of its typical values. It should be noted that only frequencies above some value ($\approx 100\ kHz$ in our case) are described by this way.

An example of the crosscorrelation function is also shown in Fig. 2b. From the time delay t_d^{MAX}, corresponding to the maximum of crosscorrelation function, the propagating velocity of the fluctuations can be estimated, $v_p = \Delta / t_d^{MAX}$.

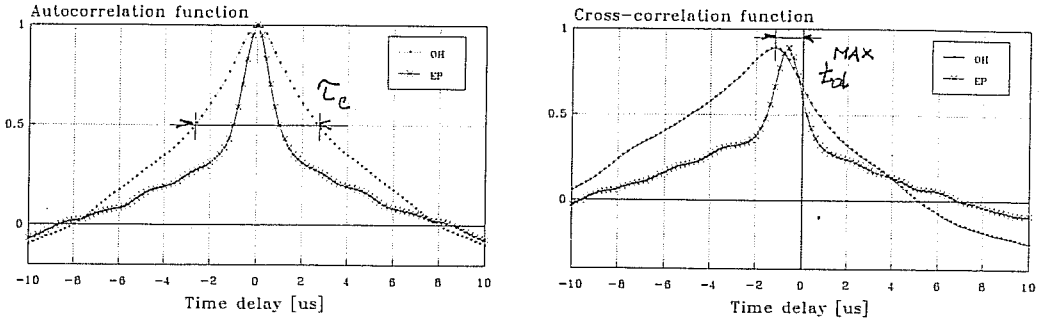

Figure 2: Auto and crosscorrelation functions of the density fluctuations.

3 Density fluctuations and global confinement

The evolutions of typical LHCD and EP shots are shown in Fig. 3.

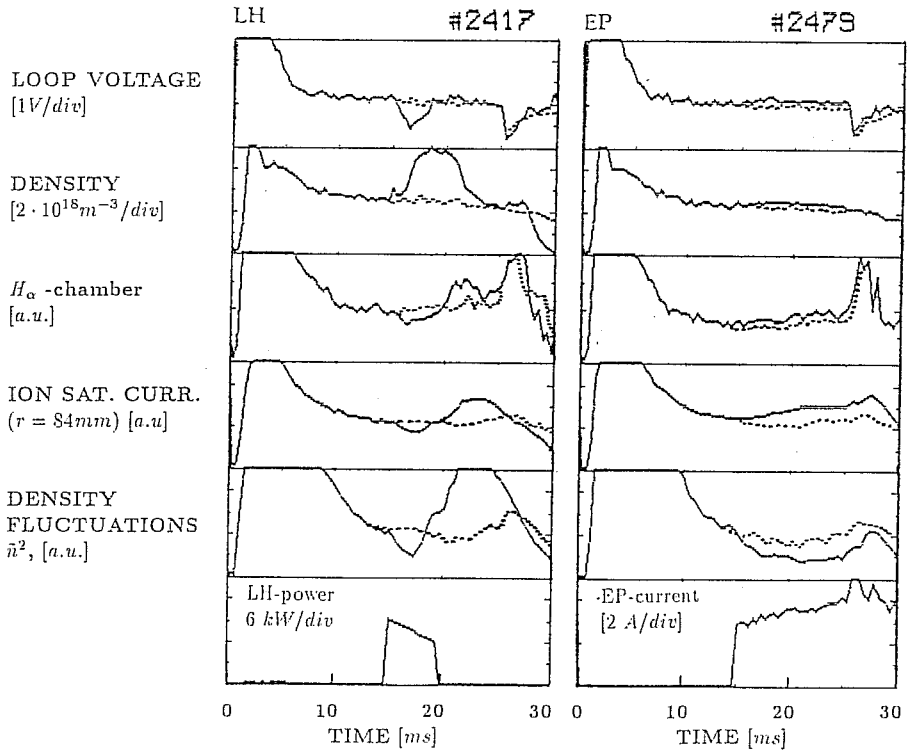

Figure 3: Temporal evolution of typical LHCD (left) and EP (right) shots. LHCD: $P_{LH} = 21\ kW$,EP: $U_b = +200\ V, r/a = 0.8$.

The characteristic drop of the loop voltage during the LH pulse, indicating the non-inductive current drive, is accompanied by a significant increase of the line average density, by broadening of its radial profile (not shown in the figure) and by a reduction of the neutral hydrogen influx (as seen from H_α line intensities). The additional ionization of impurities remains roughly on the ohmic level.

These observations are interpreted as an improvement of the particle confinement.

The detail analysis of the particle balance [9] shows that the global particle confinement time increases by a factor of 2 - 3.

On the other hand, we did not observe any significant changes in global particle confinement when the edge plasma is polarized by the biased electrode. A slight increase of the line average density is probably caused by enhanced recycling , since the H_α intensity increases during the biasing period as well. The most probable reason why neither improved confinement nor the H-mode-like transition was not observed in our case is a small active area of the graphite electrode, choosen for these preliminary experiments. Consequently, the available electrode current ($I < 10\ A$) is probably too low for an efficient plasma polarization.

At the same time, the density fluctuation are significantly reduced near LCFS in both cases. Nevertheless, the particle confinement improves only at LHCD. Suprisingly, in spite of the reduction of density fluctuations, the transport barrier is not created at the plasma edge in the EP case.

4 Correlational analysis of the density fluctuations

Radial profiles of fluctuating quantities in SOL

Radial profiles of some parameters related to the density fluctuations are compared in Fig. 4. The density fluctuations are significantly reduced in both the cases up to 50% of the standard ohmic value inside the whole scrape-off layer (SOL). The relative level of density fluctuations $\tilde{n}/n$ decreases significantly during the edge plasma polarization while it remains close to the initial value in LHCD regime.

Furthermore, we have found that the density fluctuations propagate poloidally in SOL in the ion diamagnetic drift direction consistently with the direction of the radial electric field which is positive in this region. The observed range of the velocities is from 1 to 8 km/s. We see that the shear of the poloidal velocity dv_p/dr increases, which can be a reason for damping of the fluctuations [10]. It is consistent, at least qualitatively, with the floating potential measurements [11] (performed however not in the same shot series and not in the same toroidal location), which indicate an increase of the radial electric field inside SOL in both the regimes.

For the correct interpretation of the autocorrelation measurements one has to take into account that fluctuation data in a single point in space provide an information in the laboratory frame. The width of the autocorrelation function depends not only on the real autocorrelation time in the rest (convected) frame τ_c^{conv}, but also on the correlation length λ_c and the propagation velocity v.

Transformation from laboratory to rest frame

To estimate the autocorrelation time in the rest frame, we adopt philosophy of Vayakis [12]. We consider the fluctuation field having a form of "blob" with a characteristic length $\sim \lambda_c$, which is created and destroyed in a characteristic time $\sim \tau_c^{conv}$. Such view well corresponds to a concept of well-developed turbulence in that the spatial extend of the perturbation is comparable to its "wavelength". It is consistent with direct experimental

[9] J.Badalec: This Meeting

[10] K.C. Shaing et al: Phys. Fluids, B2 (1990),1492

[11] J. Stöckel et al: IAEA TCM on Research Using Small Tokamaks, Hefei, October 1991

[12] G. Vayakis: Rep.AEA FUS 123, Coulham 1991

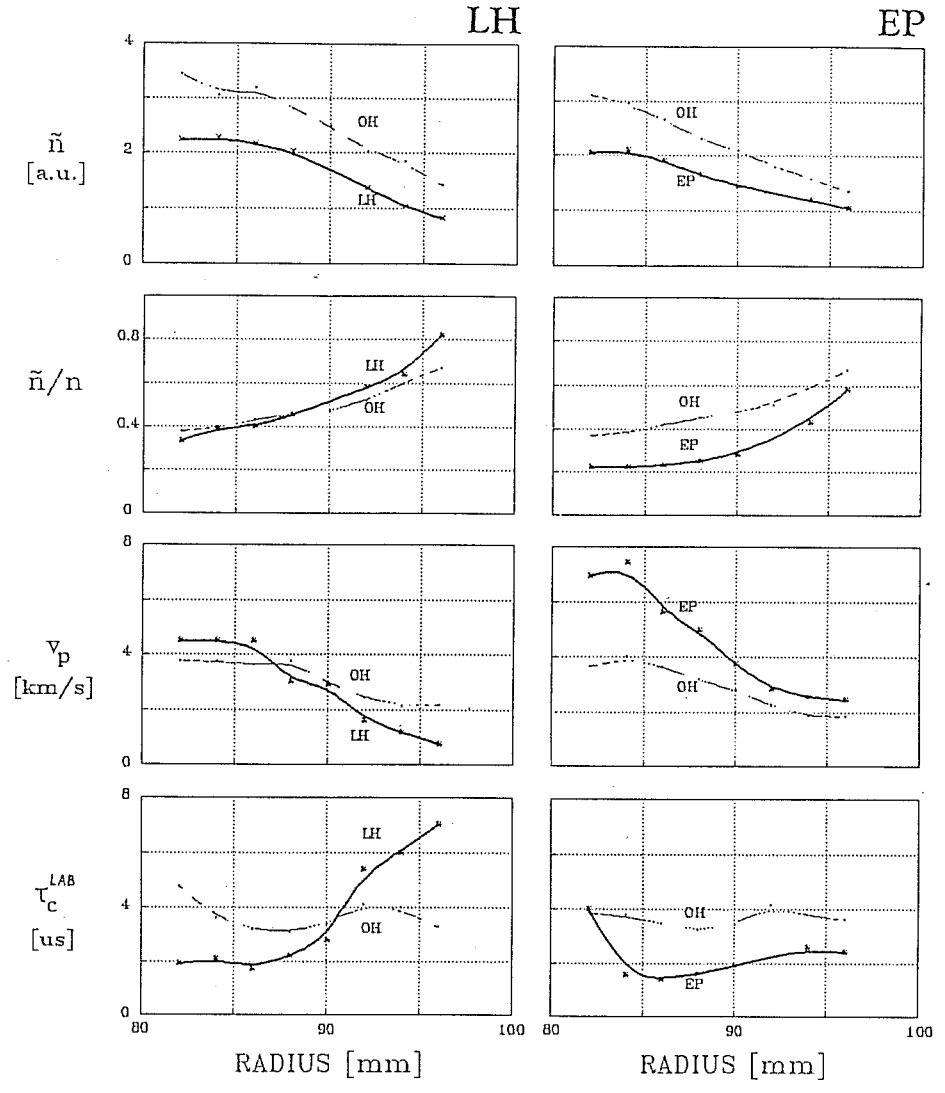

Figure 4: Comparison of radial profiles of fluctuation levels (both absolute and relative), propagation velocity in poloidal direction and the width of the autocorrelation function in OH, LHCD ($P_{LH} = 20\ kW$) and EP ($U_b = +200\ V$) regimes.

observations from the Caltech tokamak [13], which show such "blobs" being created and destroyed . Further, the functions f(x) and g(t), describing evolution of the blob in space and time, are choosen to be Gaussian.

The resulting form of the perturbing field $\phi = f(x-vt)g(t)$, measured in the laboratory frame is also Gaussian and characterized by a width τ_c^{lab}

$$\phi \equiv exp - (t/\tau_c^{lab})^2 = exp - (x - vt/\lambda_c)^2 exp - (t/\tau_c^{conv})^2 \quad .$$

Thus, the temporal width of the propagating perturbation, measured by a single probe is always shorter than the real lifetime of the blob. For the probe, located in the origin of the laboratory frame (x=0), the following relation between the parameters, characterizing the perturbation can be written:

$$(\frac{1}{\tau_c^{lab}})^2 = (\frac{1}{\tau_c^{conv}})^2 + (\frac{v}{\lambda_c})^2 \quad .$$

It has been outlined by Vayakis that the last relation is also valid for a random set of propagating perturbations. In this case, τ_c^{lab}, τ_c^{conv} mean the corresponding autocorrelation times and λ_c is the correlation length.

Fig. 5 summarizes correlation data from the radial scan of the probe in the scrape-off layer during OH , LHCD and EP shots (from Fig. 4) plotted in the scale according the last expression, to estimate the autocorrelation time unaffected by the poloidal rotation.

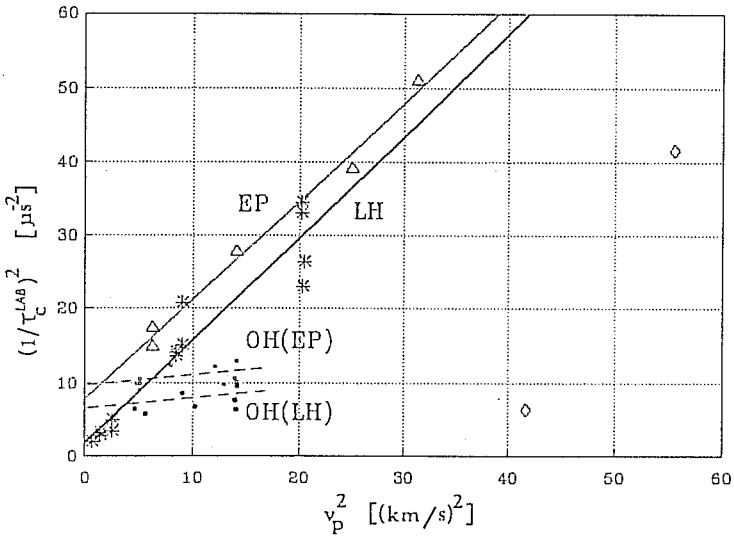

Figure 5: Plot of autocorrelation time in the lab frame versus propagation velocity of density fluctuations in scale according expression $(\frac{1}{\tau_c^{lab}})^2 = (\frac{1}{\tau_c^{conv}})^2 + (\frac{v}{\lambda_c})^2$.

It is possible to see from the plot that the experimental points are situated on lines differing in slopes and quotients. (Note, however, the two exceptional points in EP regime, which correspond to the probe positions $r < a$.) We conclude:

- Linear character of the functional dependencies $(\frac{1}{\tau_c^{lab}})^2 = f(v^2)$, apparent especialy in LHCD and EP regimes, suggests that the correlation length and time in the convected frame are constant over the whole scrape-off layer.

[13] S.J. Zweben et al: Nuclear Fusion, 25 (1985),543

- Slopes of individual lines are inversly proportional to the square of the correlation length λ_c, thus the correlation length decreases significantly in LHCD and EP regimes.

- The autocorrelation time in the rest frame can be derived from the point of intersection of the line $(\frac{1}{\tau_c^{lab}})^2 = f(v^2)$ with the y-axes. Since $(\tau_c^{conv})^{OH} < (\tau_c^{conv})^{LHCD}$, the blob lifetime increases in LHCD case. On the other hand, the blob lifetime remain unchanged when the edge plasma is polarized.

5 Dimensional analysis

Two questions about the role of the fluctuations in transport should be solved:
1) Are the fluctuations stochastic (i.e. have they a turbulent character with an infinit degrees of freedom), or are they deterministic in some way? The second possibility means that the turbulence can be described by a finit set of nonlinear equations.
2) Does the "degree of chaocity" varies when the transport properties of the tokamak plasma are changing?

This questions can be solved by computing the correlation dimension D, which represents a measure of the deterministic chaos in dynamic systems.

The correlation dimension is evaluated using the Grassberger-Procaccia algorithm [14]. From N experimental data, the n-dimensional vectors $\mathrm{r_i} = [\mathrm{x_i}, \mathrm{x_{i+d}}, ...\mathrm{x_{i+(n-1)d}}]$ are constructed, d is a time delay and n is the embedding dimension. We choose randomly a reference point $\mathrm{r_j}$ and count the number of points $\mathrm{r_i}$ inside the n-dimensional sphere of the radius r centered at the reference point $\mathrm{r_j}$. Then, after averaging over M reference points we get the correlation sum

$$C(r) = \frac{1}{M}\frac{1}{N}\sum_{j=1}^{M}\sum_{i=1}^{N}\Theta(r - |\mathrm{r_i} - \mathrm{r_j}|) \quad ,$$

which approximates the probability that two points are separated by a distance less than r. Θ is the Heaviside function. The correlation dimension $D = \lim_{r\to 0} \ln[C(r)]/\ln r$ is obtained from the slope $\ln[C(r)]$ vs $\ln r$.

The results of the dimensional analysis are shown in Fig. 6a for OH and LHCD data.

The range of embedding dimensions is $n \leq 16$, the time delay and number of reference points are choosen d=3 and M=50 respectively. In the same figure, we plot for comparison results of the calculation for random data (white noise). The correlation dimension should be equal to the embedding dimension in this case. We see, however, that $D < n$ and the difference increases with n. Therefore, the values of D for experimental data have to be taken as the lowest estimate of the correlation dimension as well.

The most important conclusion which can be drawn from the dimensional analysis is that the correlation dimension of the fluctuations in the LHCD regime is always higher than in the ohmic phase. This suggests that if the confinement improves, the fluctuations are more stochastic (closer to the white noise).

Fig 6b, where the dimensional analysis is performed for a number of LHCD shots differing by the value of LH power, documents a sufficient reproducibility of calculations (see especially values of the correlation dimension in OH phase). The correlation dimension

[14] P. Grassberger, I. Procaccia: Phys. Rev. Lett.,50,1983,346

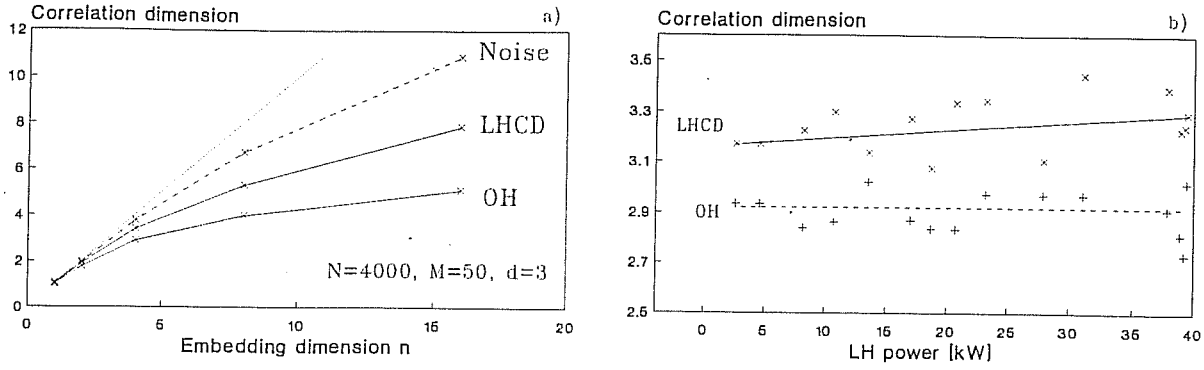

Figure 6: a) Correlation dimension of a LHCD shot (# 2425). b) Variation of the correlation dimension with LH power.

seems to be independent on the LH power consistently with former measurements on CASTOR [15].

It is interesting to note that numerical modelling of toroidal η_i mode turbulence [16] predicts a high-dimensional chaotic attractor when a regime with improved confinement (H-mode) is established.

There was a limited number of shots with the edge plasma polarization analyzed by the same way. However, due to the low statistics, we can not definitely say if the dimensionality is higher or the same with respect to the ohmic phase. The both posibilities were observed with an equal probability.

Finally, we document the proper choise of the time delay d and the number of reference points M used for the above analysis. The result of test calculations are shown in Fig. 7, where the correlation dimension is plotted for different delays and for different numbers of

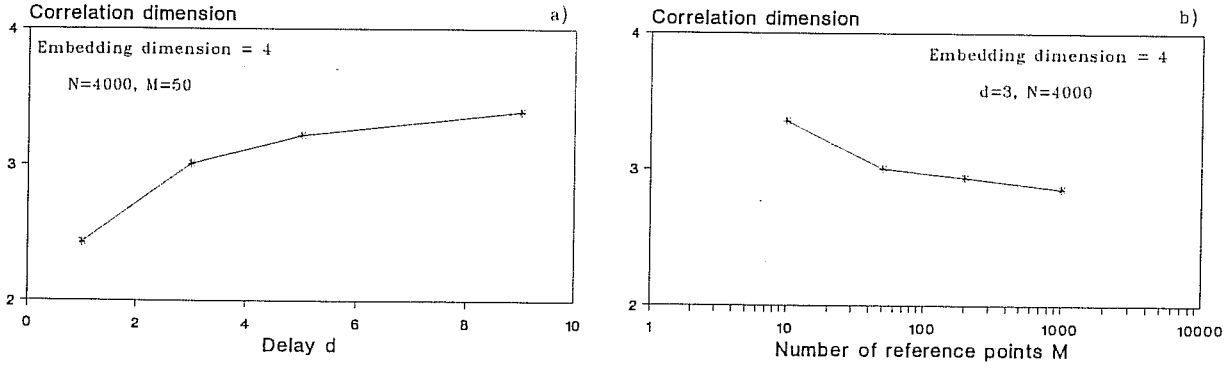

Figure 7: Test calculation of the correlation dimension for: a) different time delays d; b) for different number of reference points M.

reference points, respectively. It is evident that the choise of d and M is not too critical.

[15] F. Žáček et al: IAEA TCM on Research Using Small Tokamaks, Hefei, October 1991

[16] M. Person, H. Norman: Phys. Rev. Letters, 67,1991, No.24,p.3396

6 Summary

Two regimes with a reduced level of edge density fluctuations are compared on the CASTOR tokamak:

- Lower Hybrid Current Drive regime. The global particle confinement improves significantly with respect to the OH case when the medium LH power ($P_{LH} < P^{o}_{OH}$) is launched into the target plasma.

- Edge Plasma polarization regime. A noticeable reduction of the density fluctuations is observed inside the scrape-of-layer (SOL), however, without any influence on the global confinement properties.

It is evident from this comparison that the role of edge fluctuations in the global confinement is more complex than it is generally assumed. In fact, there is posible (but rather improbable) that the observed reduction of density fluctuations is compensated by an increase of the potential fluctuations and/or by an increase of their correlation with density fluctuations so that the fluctuation induced flux $\tilde{\Gamma}(a)$ remains unchanged. This has to be checked in next experiments.

The correlation analysis confirmed that the character of the edge fluctuations changes significantly when they are reduced. The correlation length drops in both LHCD and EP regimes. The lifetime of density perturbations increases significantly (by a factor of 3) in LHCD regimes, when also the particle confinement improves. Therefore, we conclude a link between these quantities.

The correlation dimension of the fluctuations was computed. It has been found that the fluctuations are more stochastic (close to the "white" noise), when the confinement improves.

Acknowledgement: This work was supported by the Grant of the Czech Academy of Sciences No 14310 and by the IAEA Research Contract 6702/RB.